

Transmission effects of high energy nanosecond lasers in laser-induced air plasma under different pressures

Wei-Min Hu(胡蔚敏), Kai-Xin Yin(尹凯欣), Xiao-Jun Wang(王小军), Jin Yang(杨晶), Ke Liu(刘可), Qin-Jun Peng(彭钦军), and Zu-Yan Xu(许祖彦)

Citation: Chin. Phys. B, 2023, 32 (**10**): 105201. DOI: 10.1088/1674-1056/acb0bf
Journal homepage: http://cpb.iphy.ac.cn; http://iopscience.iop.org/cpb

What follows is a list of articles you may be interested in

Theoretical analyses on the one-dimensional charged particle transport in a decaying plasma under an electrostatic field

Yao-Ting Wang(汪耀庭), Xin-Li Sun(孙鑫礼), Lan-Yue Luo(罗岚月), Zi-Ming Zhang(张子明), He-Ping Li(李和平), Dong-Jun Jiang(姜东君), and Ming-Sheng Zhou(周明胜)

Chin. Phys. B, 2023, 32 (**9**): 095201. DOI: 10.1088/1674-1056/ace033

Combination of spark discharge and nanoparticle-enhanced laser-induced plasma spectroscopy

Qing-Xue Li(李庆雪), Dan Zhang(张丹), Yuan-Fei Jiang(姜远飞), Su-Yu Li(李苏宇), An-Min Chen(陈安民), and Ming-Xing Jin(金明星)

Chin. Phys. B, 2022, 31 (**8**): 085201. DOI: 10.1088/1674-1056/ac597a

Hybrid-PIC/PIC simulations on ion extraction by electric field in laser-induced plasma

Xiao-Yong Lu(卢肖勇), Cheng Yuan(袁程), Xiao-Zhang Zhang(张小章), Zhi-Zhong Zhang(张志忠)

Chin. Phys. B, 2020, 29 (**4**): 045201. DOI: 10.1088/1674-1056/ab75d8

Damage characteristics of laser plasma shock wave on rear surface of fused silica glass

Xiong Shen(沈雄), Guo-Ying Feng(冯国英), Sheng Jing(景晟), Jing-Hua Han(韩敬华), Ya-Guo Li(李亚国), Kai Liu(刘锴)

Chin. Phys. B, 2019, 28 (**8**): 085202. DOI: 10.1088/1674-1056/28/8/085202

Conditions for laser-induced plasma to effectively remove nano-particles on silicon surfaces

Jinghua Han(韩敬华), Li Luo(罗莉), Yubo Zhang(张玉波), Ruifeng Hu(胡锐峰), Guoying Feng(冯国英)

Chin. Phys. B, 2016, 25 (**9**): 095204. DOI: 10.1088/1674-1056/25/9/095204

Transmission effects of high energy nanosecond lasers in laser-induced air plasma under different pressures

Wei-Min Hu(胡蔚敏)[1,2,3], Kai-Xin Yin(尹凯欣)[1,2,†], Xiao-Jun Wang(王小军)[1,2], Jing Yang(杨晶)[1,2], Ke Liu(刘可)[1,2], Qin-Jun Peng(彭钦军)[1,2], and Zu-Yan Xu(许祖彦)[1,2]

[1] *Key Laboratory of Solid State Lasers, Technical Institute of Physics and Chemistry, Chinese Academy of Sciences, Beijing* 100190, *China*
[2] *Institute of Optical Physics and Engineering Technology, Qilu Zhongke, Jinan* 250000, *China*
[3] *University of Chinese Academy of Sciences, Beijing* 100049, *China*

(Received 23 November 2022; revised manuscript received 4 January 2023; accepted manuscript online 6 January 2023)

When a high energy nanosecond (ns) laser induces breakdown in the air, the plasma density generated in the rarefied atmosphere is much smaller than that at normal pressure. It is associated with a relatively lower absorption coefficient and reduces energy loss of the laser beam at low pressure. In this paper, the general transmission characterizations of a Joule level 10 ns 1064 nm focused laser beam are investigated both theoretically and experimentally under different pressures. The evolution of the electron density (n_e), the changes in electron temperature (T_e) and the variation of laser intensity (I) are employed for numerical analyses in the simulation model. For experiments, four optical image transfer systems with focal length (f) of 200 mm are placed in a chamber and employed to focus the laser beam and produce plasmas at the focus. The results suggest that the transmittance increases obviously with the decreasing pressure and the plasma channels on the transmission path can be observed by the self-illumination. The simulation results agree well with the experimental data. The numerical model presents that the maximum n_e at the focus can reach 10^{19} cm^{-3}, which is far below the critical density (n_c). As a result, the laser beam is not completely shielded by the plasmas.

Keywords: laser-induced plasma, high energy, nanosecond laser pulse, rarefied atmosphere

PACS: 52.38.Dx, 42.25.Bs, 52.38.–r, 52.80.Mg **DOI:** 10.1088/1674-1056/acb0bf

1. Introduction

Recently, many groups have studied the transmission effects of the high energy short pulse laser in the atmosphere,[1–11] which is useful for some technical fields, such as directed energy systems,[12] laser lightning rods,[13] atmospheric laser communication,[14] laser radar,[15] etc.

As is well known, the nonlinear effects, such as Kerr self-focusing and plasma defocusing, can be generated when an intense enough laser with short pulse duration propagates through air. Kerr self-focusing will be the result when the laser power reaches its threshold, which further increases the laser intensity (I) undoubtedly. The propagation mentioned above triggers the multiphoton ionization (MPI) and cascade ionization (CI) to generate electrons and ions.[16] The breakdown happens when the I reaches the threshold, which means that the electron density (n_e) is strengthened to a magnitude of $\sim 10^{13} \times n_{e0}/\text{cm}^3$ (n_{e0} is the natural electron density) and an intense spark (plasmas) is formed.[17] Because of the complex recombination processes, the plasmas can be observed by its self-illumination.[7] However, plasmas generated by the pulse negatively affect the refractive index, which defocuses the laser beam and absorbs the laser energy.[2,3] It is well known that the absorption coefficient can be extremely high when the n_e is large enough, and the laser beam will be attenuated rapidly in plasmas.[18] To our knowledge, most previous reports used the femtosecond (fs) lasers to study the transmission effects.[1–3] This is because the pulse duration of the fs laser is similar to the time for forming plasmas, which allows the pulse to propagate through a long distance with less assimilation. Unlike the fs laser, however, when a high energy nanosecond (ns) laser is focused by a single lens in normal air, the plasmas generated at the focal region strongly absorb the energy. In this case, the ns laser barely gets out of the plasma region due to long pulse duration and huge absorption coefficient, so that the I at the focus is seriously affected. Theoretically, the plasma density induced by a high energy ns laser in the rarefied atmosphere is much smaller than that at normal pressure, which is correlated to a relatively lower absorption coefficient and reduces energy loss of the laser beam.[5,6] In this paper, the transmission characterizations of a Joule level 10 ns 1064 nm focused laser beam are investigated both in theory and experiment under different pressures. The key physical quantities are discussed in the numerical simulation. For the experiment section, 10 ns pulses from a Q-switched Nd:YAG laser (model number: SGR Extra-10) transmit through four optical image transfer systems with focal length (f) of 200 mm in an aluminum alloy chamber, with air pressure of 5–760 Torr. The simulation results show a good agreement with the experimental data. For the incident energy of 6 J, the transmitted energy after passing through the chamber is 3.4±0.1 J at 5 Torr. The maximum n_e at the

[†]Corresponding author. E-mail: yinkx@mail.ipc.ac.cn

© 2023 Chinese Physical Society and IOP Publishing Ltd

first focus is calculated as 2.4×10^{19} cm^{-3}. Additionally, the transmittance and the average n_e along the transmission path in the first optical image transfer system ($\bar{n}_e$) versus light intensity at the first focus without absorption (I_0) and pressure are detailed discussed. Moreover, the transmission effects of picosecond (ps) pulsed laser can be predicted by using the numerical model.

2. Theoretical model

The theoretical simulation focuses on the propagation of a 10 ns pulse 1064 nm laser beam in air. Some parameters are discussed, including the n_e, the electron temperature T_e and the variation of I. It is assumed that the laser beam exhibits a fundamental-mode Gaussian distribution and the propagation is one-dimensional (1D). Additionally, the air is assumed to comprise 80% nitrogen and 20% oxygen in this paper. The n_{e0} at normal pressure is defined as 10^3 cm^{-3} and it reduces linearly with pressure.[17]

The atoms in a powerful laser field can absorb multiple photons to achieve the transition, thereby shifting from the ground or excited states to the continuous state and producing MPI. The electrons generated by MPI or existing in air are heated by the laser field, and then collide with neutral gas molecules, resulting in CI. As a joint result of these two kinds of ionization and electron recombination process, the growth of n_e can be described by the following equation:[16]

$$\frac{\partial n_e}{\partial t} = \frac{NA}{K^{3/2}} I^K + n_e N \left[\frac{377q}{\omega^2}\left(\frac{\nu_m}{N}\right)^2\right] I - \alpha n_e^2. \tag{1}$$

The first term in Eq. (1) represents the MPI process. K is the number of photons required for multiphoton ionization of the gas. N is the neutral atom density of the gas ($N = 3.56\times10^{16}P$ cm^{-3}, where P is the pressure in Torr). A represents the multiphoton absorption coefficient, which can be defined by the following expression:[16]

$$A = \frac{\sigma^K}{\nu^{K-1}(K-1)!(h\nu)^K}, \tag{2}$$

where the photoionization cross section σ is set as $10^{-17\pm1}$ cm^2,[16,19] ν is the frequency of the laser beam, and $h\nu$ refers to the energy of the single photon. The second term in Eq. (1) describes the CI process, where q is a constant for a particular gas, ω is the angular frequency of the laser and ν_m refers to the frequency of the electron momentum transfer collision. The third term in Eq. (1) expresses the radiative electron recombination, where α is the coefficient, which is determined by T_e.[20]

When the contribution of MPI and plasmas for absorbing energy of laser through transmitting procedure are considered, the variation of I with distance can be given as follows:[3,18,21]

$$\frac{dI}{dz} = -\kappa_{ib} I - h\nu NAKI^K. \tag{3}$$

In Eq. (3), κ_{ib} is the inverse bremsstrahlung absorption coefficient of plasma, which is written as[18]

$$\kappa_{ib} = \frac{\nu_{ei}(n_c)}{c}\left(\frac{n_e}{n_c}\right)^2\left(1-\frac{n_e}{n_c}\right)^{-\frac{1}{2}}. \tag{4}$$

In the above equation, n_c is the critical density for a laser beam, which is inversely proportional to the square of the laser wavelength (λ).[18] Normally, when $n_e \geq n_c$, the plasmas exert a severe shielding role on the laser beam and a negative effect on the transmission. Besides, ν_{ei} represents the frequency of electron ion collision, which is described as follows:[18]

$$\nu_{ei} \approx 2.9\times10^{-6}\frac{Z^2 n_e \ln\Lambda}{[T_e(\mathrm{eV})]^{\frac{3}{2}}}. \tag{5}$$

In Eq. (5), Z represents the charge number of an ion. Λ is the Coulomb cutoff coefficient. T_e refers to the electron temperature, which is determined with the Saha–Eggert equation and written as follows:[18]

$$\frac{Z_l^2}{1-Z_l} \approx \frac{2}{N}\left(\frac{2\pi m_e k_B T_e}{h^2}\right)^{\frac{3}{2}} \exp\left(\frac{-W_{ion}}{k_B T_e}\right), \tag{6}$$

where $Z_l = n_e/N$ is the degree of ionization, m_e is the mass of electron. W_{ion} represents the ionization potential, which normally is 15.6 eV for nitrogen and 12.1 eV for oxygen. k_B stands for the Boltzmann constant.

Usually, the Kerr self-focusing occurs when the laser power is higher than the critical value $P_{cr} = 3.77\lambda^2/(8\pi n_0 n_2)$, in which n_2 is the nonlinear refractive index, which is 5×10^{-19} cm^2/W for normal air and 1×10^{-34} cm^2/W for vacuum.[22] $n_0 = 1$ is the linear refractive index of the medium. It has been reported that the n_2 of air depends linearly on pressure.[23–25] As a result, $P_{cr} \approx 3.4$ GW at atmospheric pressure and P_{cr} increases with decreasing pressure. In this paper, the incident power of the laser is lower than 1 GW, which means that the self-focusing can be neglected. The numerical results of the transmission effects at different pressures can be obtained by solving the above equations with the finite difference method.

3. Experiment setup

Figure 1 shows the schematic diagram of the experimental system. A Q-switched Nd:YAG laser is employed to generate the 10 ns 1064 nm laser pulses (red lines in Fig. 1). With the assistance of a control panel, the single pulse is emitted in each experiment and the maximum energy can reach 10 J. The initial radius of the beam is about 15 mm and the beam quality factor (β) is about 1.7. In the experiment, the radius of the beam is reduced to 7.5 mm by using a positive lens ($f = 1000$ mm) and a negative lens ($f = -500$ mm). The radius of focus (r) is calculated to be 28 μm. The aluminum

alloy chamber in Fig. 1 is filled with air, and its pressure of 5–760 Torr. To prolong the plasma generation region and increase the the absorptivity of pulse, four optical image transfer systems (f = 200 mm), consisting of eight focal lenses and placed side-by-side, are adopted to focus the laser pulse four times and produce four small plasma channels. The plasma generation region is enclosed by the dashed lines in Fig. 1. The plasma channels can be observed due to its self-illumination. The transmitted energy via the chamber is measured with an energy meter. After the inherent loss of the chamber is subtracted, the incident energy of laser pulses in experiments is 1.4 J, 2.9 J, 4.5 J, and 6.0 J, respectively. For a Gaussian beam, the effective area is equal to $\pi r^2/2$. Therefore, the I_0 can reach 11.4 TW/cm^2, 23.5 TW/cm^2, 36.5 TW/cm^2, and 48.7 TW/cm^2, respectively. In contrast with the experimental data in the previous literature (for 6 ns single pulse, the breakdown threshold is 0.2 TW/cm^2 at 760 Torr and 3 TW/cm^2 at 10 Torr),[5] the I_0 here is large enough to generate the plentiful plasmas and absorb the energy.

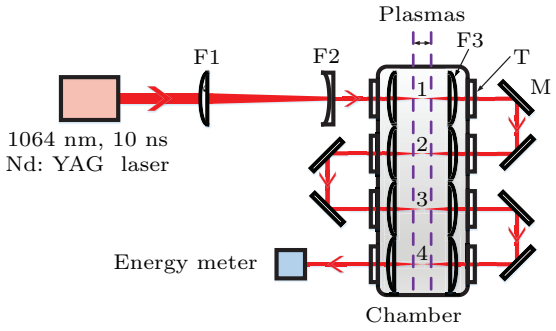


Fig. 1. Schematic diagram of the experimental system. F1–F3 are the focal lens with the f of 1000 mm, −500 mm, and 200 mm, respectively). T is the transmission window. M is the 45° high reflective mirrors. Numbers 1–4 represent four independent plasma channels.

4. Results and discussion

Figure 2 describes the two typical plasma channels (the first and second channel in Fig. 1) recorded by two cameras at the pressure of 5 Torr and the incident energy of 6 J. The total length and diameter of four channels is 3.5 cm and 0.17–0.3 cm, respectively. The energy meter shows that the transmitted energy is 3.4±0.1 J. Meanwhile, the simulation results indicate that the transmitted energy is about 3.3 J and the maximum n_e at the first focus is 2.4×10^{19} cm^{-3}. As demonstrated in Fig. 2, the first channel lies more left than the second one, which is caused by the transmission path of the laser. The breakdown initiates at a location before the focus of the focal lens, and the breakdown-induced plasmas begin to spread. The backward moving plasmas (toward the lens) absorb the remnant energy of the incident laser pulse and exhibit a more obvious growth trend when compared with the forward-moving plasmas (away from the lens).[26]

The transmitted energies for the 1.4 J laser pulses passing through the chamber at different pressures are shown in Fig. 3. It suggests that the transmitted energy is increased with the reducing pressure and the energy changes with log base 10 of pressure approximately linearly when the pressure ranges from 30–350 Torr. However, the transmitted energy declines slowly with the increasing pressure after it is higher than 350 Torr. This is because the n_e is relatively small at the initial stage of the Gaussian pulse, which cannot disturb the energy so that the front part of the pulse transmits through the chamber. In addition, the error bars are much longer in the middle parts than that in the marginal parts, which may be attributed to the following two aspects. Firstly, the gas molecules are unevenly distributed, causing different results for repeated experiments. Then, the experimental data may be influenced by some aerosols with the breakdown threshold of 10^8 W/cm^2, which is far below the threshold of the air.[27] When the pressure approaches to the atmospheric pressure, both aerosols and air can be easily breakdown. However, there are almost no aerosols at low pressure. As a result, the error bars at these two parts are relatively shorter.

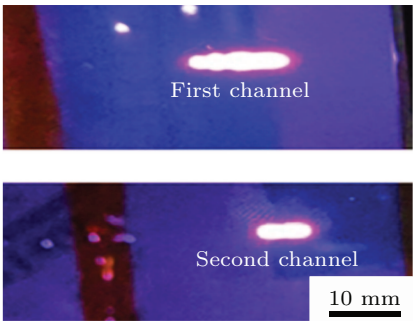


Fig. 2. Images of two plasma channels generated by the first and second image transfer systems in Fig. 1, the pressure is 5 Torr and the incident energy is 6 J.

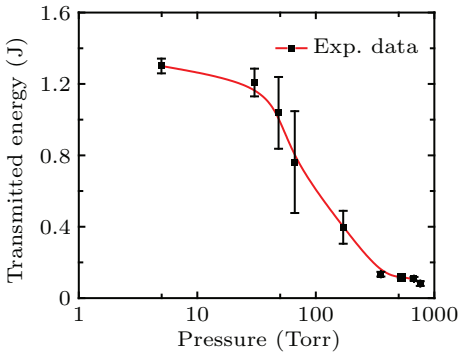


Fig. 3. Transmitted energies of 1.4 J incident energy versus pressure.

Figure 4(a) shows the experimental and numerical results of the transmittance versus I_0 under different pressures. Solid stars and error bars represent the experimental data, and solid lines are selected to mark the numerical results. According to Eq. (1), the breakdown threshold increases as the pressure decreases. When the I_0 is 11.4 TW/cm^2, the intensity is not high enough to excite more plasmas to absorb the energy at low pressures. Therefore, the transmittance in

this situation approaches to 100%. Meanwhile, it suggests that the experimental data are slightly lower than the theoretical results. It can be inferred that the diffusion of plasmas, which is not considered in the numerical model, increases the energy loss in the experiments. To investigate the effects of the n_e on absorption, the maximum n_e during the transmission is calculated, which can reach 10^{17}–10^{19} cm^{-3} in the experiments. However, the n_e at the focal region under the high-pressure air has to be considered, because it is large enough to severely influence the energy. After the n_e along the transmission path is integrated, the average n_e is calculated. Figure 4(b) shows the $\bar{n}_e$ versus I_0 under different pressures in the simulation model. The variation tendency of the $\bar{n}_e$ is observed to be opposite to the transmittance. This is because a larger I_0 can generate more plasmas at high pressure, which absorbs more energy and seriously affects the transmittance. Due to different pressures and incident energies, the plasma channels present various total lengths. For example, the channel is 2.1 cm in length when the pressure is 50 Torr and the I_0 is 11.4 TW/cm^2, but it can be 10.6 cm when the pressure is 30 Torr and the I_0 is 48.7 TW/cm^2. Furthermore, no self-illumination is found at the pressure of 5 Torr and I_0 of 11.4 TW/cm^2 in the experiment. Whereas the transmitted energy is slightly lower than the incident energy under the same conditions. It indirectly proves that the total length of the plasma channel is longer than that of the self-illumination due to its invisible part, which is consistent with the findings in a previous study.[28] Additionally, the results in Fig. 4 can be based to estimate the transmittance and n_e of the laser pulse with pulse duration larger than the time of plasma generation ($\sim$ 10 ps) under different atmospheric pressures.

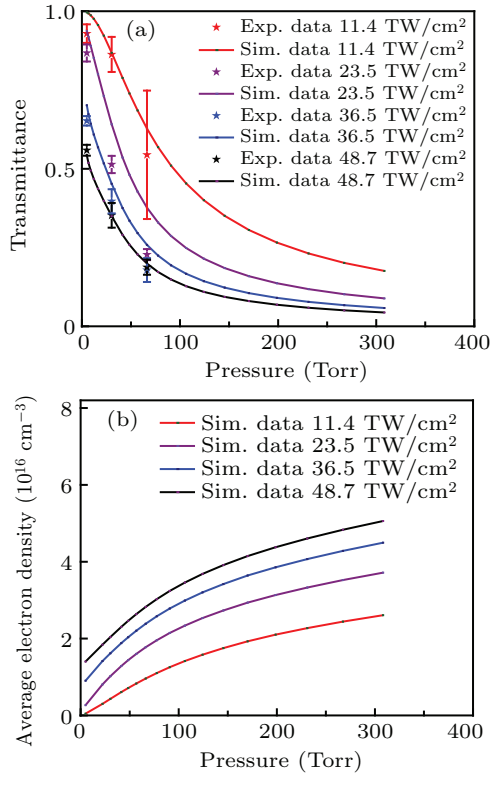


Fig. 4. (a) Transmittance and (b) $\bar{n}_e$ versus I_0 and pressure (5–310 Torr).

5. Conclusion

The transmission characterizations of a Joule level 10 ns 1064 nm focused laser beam in the atmosphere with different pressures are theoretically and experimentally analyzed in this paper. A 10 ns pulse from a Q-switched Nd:YAG laser is transmitted through four optical image transfer systems inside a chamber, with the pressure ranges from 5–760 Torr. The shapes of the plasma channels are photographed, and the numerical results agree well with the experimental data. At the pressure of 5 Torr and the incident energy of 6 J, the transmitted energy passing through the chamber is 3.4 ± 0.1 J and the maximum n_e at the first focus is 2.4×10^{19} cm^{-3}. Additionally, the transmittance and the $\bar{n}_e$ during the propagation are detailed analyzed. Furthermore, the theoretical model is employed to predict the transmission effects of ps pulsed laser in the air. For example, when a 10 ps pulse with energy of 6 mJ transmits through the experimental system at 5 Torr, the transmittance and maximum n_e are 55.87% and 4.5×10^{19} cm^{-3}, respectively.

Acknowledgement

Project supported by the Science and Technology Innovation Foundation of the Chinese Academy of Sciences (Grant No. CXJJ-20S020).

References

[1] Shu X F, Yu C X, Li W and Liu S B 2015 *Phys. Rev. A* **92** 063844
[2] Chen S Y, Teng H, Lu X, Shen Z W, Qin S, Wei W S, Chen R Y, Chen L M, Li Y T and Wei Z Y 2018 *Chin. Phys. B* **27** 085203
[3] Feng Z F, Li R, Li W, Liu Y, Shu X F, Yu C X, Li J H and Liu X 2022 *Opt. Commun.* **502** 127404
[4] Soubacq S, Pignolet P, Schall E and Batina J 2004 *J. Phys. D: Appl. Phys.* **37** 2686
[5] Thiyagarajan M and Thompson S 2012 *J. Appl. Phys.* **111** 073302
[6] Zhang H T, Sun H, Wu Y and Zhou Q H 2021 *Spectrochimica Acta B* **177** 106103
[7] Böker D and Brüggemann D 2011 *Spectrochimica Acta B* **66** 28
[8] Mahdieh M H and Jafarabadi M A 2015 *Phys. Plasmas* **22** 123117
[9] An B, Wang Z G, Yang L C, Wu G, Zhu J J and Li X P 2017 *J. Appl. Phys.* **122** 193301
[10] Nagli L, Gaft M and Raichlin Y 2019 *Opt. Commun.* **443** 63
[11] Wang X S, Song X W, Gao X and Lin J Q 2020 *Opt. Commun.* **456** 124603
[12] Zhang Y X, Zhu Z, Joseph R and Shihan I J 2021 *Defence Technology* **17** 1269
[13] Produit T, Walch P, Herkommer C, Mostajabi A, Moret M, Andral U, Sunjerga A, Azadifar M, André Y B, Mahieu B, Haas W, Esmiller B, Fournier G, Krötz P, Metzger T, Michel K, Mysyrowicz A, Rubinstein M, Rachidi F, Kasparian J, Wolf J P and Houard A 2021 *Eur. Phys. J. Appl. Phys.* **93** 10504
[14] Wang T, Zhao X, Song Y S, Wang J Y, Yu X N and Zhang Y Q 2017 *IEEE Access* **9** 43339
[15] Song W H, Ghassemlooy Z, Lai J C, Yan W, Wang C Y and Li Z H 2017 *J. Opt.* **19** 045605
[16] Sircar A, Dwivedi R K and Thareja R K 1996 *Appl. Phys. B* **63** 623

[17] Hermann J and Floch T L 2004 *J. Appl. Phys.* **96** 3084
[18] Eliezer S 2002 *The Interaction of High-Power Lasers with Plasmas* (London: The Institute of Physics Publishing) pp. 23–86
[19] Gamal Y E E D, Shafik M S E D and Daoud J M 1999 *J. Phys. D: Appl. Phys.* **32** 423
[20] Zhao X M, Diels J C, Wang C Y and Elizondo J M 1995 *IEEE J. of Quantum Electronics* **31** 599
[21] Zhang Z M and Chen D H 2002 *J. Heat Trans.* **124** 391
[22] Boyd R W 2008 *Nonlinear Optics*, 3rd edn. (New York: Academic Press) p. 213
[23] Shimoji Y, Fay A T, Chang R S F and Djeu N 1989 *J. Opt. Soc. Am. B* **6** 1994
[24] Börzsönyi Á, Heiner Z, Kovács A, Kalashnikov M P and Osvay K 2009 *Nonlinear Photonics.*
[25] Börzsönyi Á, Heiner Z, Kovács A, Kalashnikov M P and Osvay K 2010 *Opt. Express* **18** 25847
[26] Bindhu C V, Harilal S S, Tillack M S, Najmabadi F and Gaeris A C 2003 *J. Appl. Phys.* **94** 7402
[27] Shimada Y, Uchida S, Yasuda H, Motokoshi S, Yamanaka C, Kawasaki Z, Yamanaka T, Ishikubo Y and Adachi M 1998 *Proc. SPIE* **3423** 258
[28] Zhong J Y, Li Y T, Lu X, Zhang Y, Jens B, Liu F, Hao Z Q, Zhang Z, Yu Q Z, Chen M, Yuan X H, Liang W X, Zhao G and Zhang J 2007 *Acta Phys. Sin.* **56** 7114 (in Chinese)